Nuclear magnetic resonance study of hydrogen diffusion in A15-type $Nb_3AlH_x$



2000 J. Phys.: Condens. Matter 12 9607

(http://iopscience.iop.org/0953-8984/12/46/308)

J. Phys.: Condens. Matter **12** (2000) 9607–9616. Printed in the UK PII: S0953-8984(00)15727-3

# Nuclear magnetic resonance study of hydrogen diffusion in A15-type $Nb_3AlH_x$

A V Skripov, A V Soloninin, A P Stepanov and V N Kozhanov

Institute of Metal Physics, Urals Branch of the Academy of Sciences, Ekaterinburg 620219, Russia

Received 20 July 2000, in final form 25 September 2000

**Abstract.** Nuclear magnetic resonance measurements of the proton spin–lattice relaxation rate $T_1^{-1}$ for A15-type $Nb_3AlH_x$ ($x = 0.13$, 1.77 and 2.75) have been performed over the temperature range 20–420 K and the resonance frequency range 13–90 MHz. The experimental results are analysed to evaluate the electronic (Korringa) contributions to $T_1^{-1}$ and the parameters of hydrogen diffusion. It is found that the electronic contribution to the relaxation rate decreases with increasing H content. The effective activation energies for H diffusion derived from the high-temperature relaxation rate data are 0.21 eV for $x = 0.13$ and 0.30 eV for $x = 1.77$ and 2.75. The behaviour of $T_1^{-1}$ at low temperatures ($T < 270$ K for $x = 1.77$ and 2.75) suggests a coexistence of at least two frequency scales of H hopping. It is shown that the structure of the sublattice of interstitial d sites (partially occupied by hydrogen) is consistent with the coexistence of two characteristic jump rates for H atoms.

## 1. Introduction

The cubic A15-type intermetallic compounds $A_3B$ show a number of unusual electron and phonon properties [1,2]. Some of the A15-type compounds (mostly, those with A = Nb and Ti) can absorb large amounts of hydrogen [3–10]. The host lattice usually retains the A15 structure upon hydrogen absorption. Previous studies of the effects of hydrogen in A15 materials were devoted mainly to its impact on the superconducting transition temperature $T_c$ [3–6, 8, 11]. However, little is known about the hydrogen mobility and the mechanisms of H diffusion in these compounds. Microscopic information on H motion can be obtained from nuclear-magnetic-resonance (NMR) measurements of the proton spin–lattice relaxation time $T_1$ [12]. Proton NMR studies of H mobility have been reported for the A15-type hydrides $Ti_3IrH_x$ [13], $Ti_3SbH_x$ [14] and $V_3GaH_x$ [15]. For all of these systems the measured temperature dependence of the proton spin–lattice relaxation rate $T_1^{-1}$ shows a characteristic maximum. This maximum is known to result from the dipole–dipole interactions between nuclear spins; it occurs at the temperature $T_{max}$ at which $\omega_H \tau_d \approx 1$, where $\omega_H$ is the $^1H$ resonance frequency and $\tau_d$ is the mean residence time of a hydrogen atom at an interstitial site. Such a maximum is a common qualitative feature of the proton spin–lattice relaxation data for metal–hydrogen systems [12]. It should be noted, however, that the detailed analysis of the $T_1^{-1}(T)$ results for $Ti_3SbH_x$ [14] and $V_3GaH_x$ [15] has revealed strong deviations of the observed behaviour of $T_1^{-1}$ from that expected for conventional models with the Arrhenius-like temperature dependence of $\tau_d$. Moreover, for these systems the spin–lattice relaxation data appear to be consistent with a coexistence of at least two frequency scales of the hydrogen hopping rate $\tau_d^{-1}$. The origin of the two frequency scales has not been elucidated unambiguously. The aim of the present

0953-8984/00/469607+10$30.00  

work is to determine the parameters of hydrogen diffusion in the niobium-based A15-type system $Nb_3Al$–H using the proton $T_1^{-1}$-measurements. From the NMR point of view, the advantage of this system is related to the fact that dipole–dipole interactions for proton spins in $Nb_3AlH_x$ are dominated by strong $^1H$–$^{93}Nb$ interactions. This is expected to result in high maximum values of $T_1^{-1}$, i.e. in a large dynamic range for the dipolar contribution to $T_1^{-1}$, which is favourable for data analysis. X-ray diffraction studies of $Nb_3AlH_x$ [5] at room temperature have shown that in the hydrogen concentration range $0.2 \leqslant x \leqslant 1.5$ there are two coexisting phases with the same A15-type host lattice, but with different lattice parameters. A single-phase state of $Nb_3AlH_x$ with the A15-type host lattice has been found for $x < 0.2$ and $1.5 < x \leqslant 2.2$ [5]. To the best of our knowledge, there is no direct information on the positions occupied by hydrogen in $Nb_3Al$. However, on the basis of the general trends of site occupancy in hydrides of intermetallic compounds [16] and the neutron diffraction data for A15-type $Nb_3SnH_{1.0}$ [4], $Ti_3SbD_{2.6}$ [17], $Ti_3IrD_x$ [18] and $Nb_3AuH_x$ [19], we may expect H atoms in $Nb_3AlH_x$ to occupy the 6d positions of the space group $Pm\bar{3}n$ (i.e. the tetrahedral interstitial sites formed by four Nb atoms). In the present work we report the results of the proton $T_1^{-1}$-measurements for $Nb_3AlH_x$ ($x = 0.13$, 1.77 and 2.75) over wide ranges of the temperature and the resonance frequency. The experimental results are analysed to determine the electronic (Korringa) contributions to $T_1^{-1}$ and the parameters of hydrogen diffusion.

## 2. Experimental details

The $Nb_3Al$ compound was prepared by arc melting of high-purity Nb and Al in a helium atmosphere. The resulting single-phase material had the A15-type structure with the lattice parameter $a_0 = 5.187$ Å. Small pieces of $Nb_3Al$ were charged with hydrogen at a pressure of about 1 bar using a Sieverts-type vacuum system. After annealing the sample in vacuum at 700 °C, the calculated amount of $H_2$ gas was admitted to the system at this temperature, and the sample was slowly cooled to room temperature (for about 8 h) in a hydrogen atmosphere. The hydrogen content of the sample was determined from the pressure change in the calibrated volume of the system. Four $Nb_3AlH_x$ samples with the nominal hydrogen contents $x = 0.13$, 1.06, 1.77 and 2.75 were prepared. According to x-ray diffraction analysis, the samples of $Nb_3AlH_{0.13}$, $Nb_3AlH_{1.77}$ and $Nb_3AlH_{2.75}$ were single-phase compounds having A15-type host-metal structure with $a_0 = 5.190$, 5.353 and 5.358 Å, respectively. The $Nb_3AlH_{1.06}$ sample was found to contain two coexisting A15-type phases with $a_0 = 5.198$ and 5.352 Å. This is consistent with the results of [5] showing the two-phase region for $Nb_3AlH_x$ with $0.2 \leqslant x \leqslant 1.5$. NMR measurements were made on the powdered single-phase samples of $Nb_3AlH_x$ ($x = 0.13$, 1.77 and 2.75) using a modernized Bruker SXP pulse spectrometer. Proton spin–lattice relaxation rates were measured by the saturation–recovery method at the frequencies $\omega_H/2\pi = 13$, 23.8, 40 and 90 MHz. In all cases the recovery of the nuclear magnetization could be fitted with a single exponential function.

## 3. Results and discussion

The results of the proton spin–lattice relaxation rate measurements for $Nb_3AlH_{0.13}$, $Nb_3AlH_{1.77}$ and $Nb_3AlH_{2.75}$ are shown in figures 1, 2 and 3. For the sample with $x = 0.13$ the relaxation rate has been measured only at the frequencies of 40 and 90 MHz, since at lower frequencies the observed proton NMR signal appears to be weak. As can be seen from figures 1–3, the dominant feature of the data is the frequency-dependent relaxation rate peak which is typical for the mechanism of the dipole–dipole interaction modulated by atomic motion. As the hydrogen

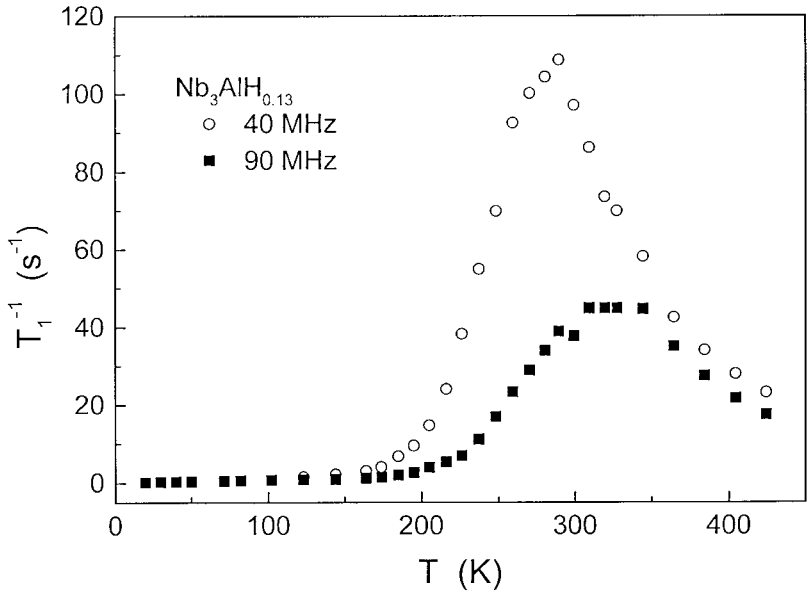


**Figure 1.** The temperature dependence of the proton spin–lattice relaxation rate for $Nb_3AlH_{0.13}$ measured at 40 and 90 MHz.

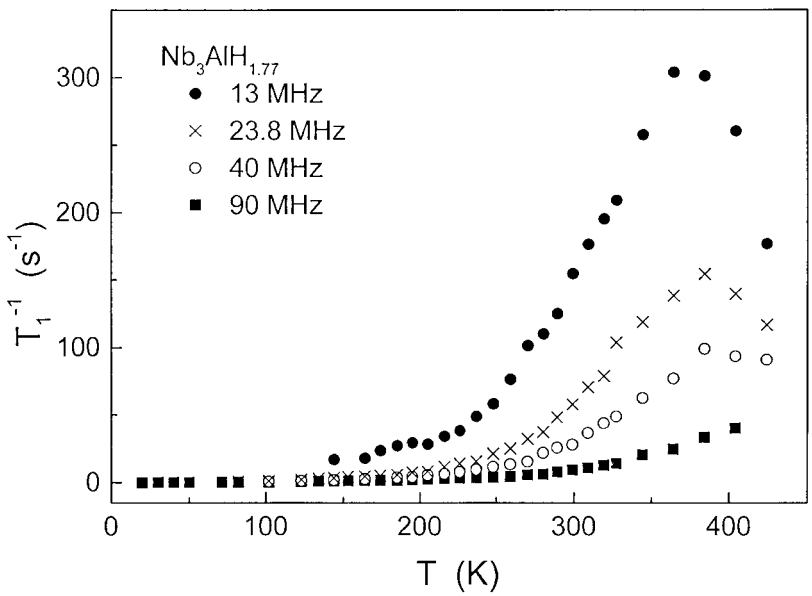


**Figure 2.** The temperature dependence of the proton spin–lattice relaxation rate for $Nb_3AlH_{1.77}$ measured for 13, 23.8, 40 and 90 MHz.

content increases, the peak position is shifted to higher temperatures. The amplitude of this peak is nearly $x$-independent. In order to evaluate the parameters of hydrogen motion, we have to separate contributions of different natures to $T_1^{-1}$. The measured proton spin–lattice

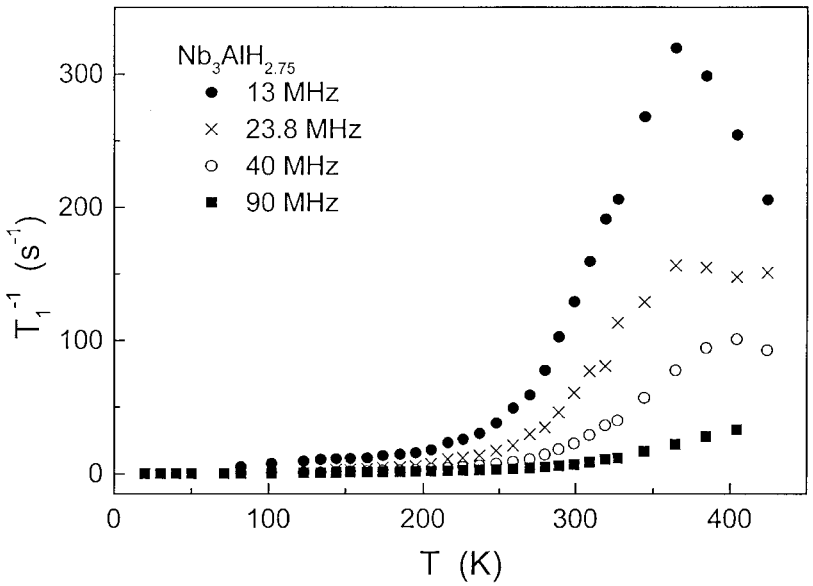


**Figure 3.** The temperature dependence of the proton spin–lattice relaxation rate for $Nb_3AlH_{2.75}$ measured at 13, 23.8, 40 and 90 MHz.

relaxation rate for metal–hydrogen systems usually results from the sum of contributions due to conduction electrons ($T_{1e}^{-1}$), paramagnetic impurities ($T_{1p}^{-1}$) and the internuclear dipole–dipole interaction modulated by H motion ($T_{1d}^{-1}$):

$$T_1^{-1} = T_{1e}^{-1} + T_{1p}^{-1} + T_{1d}^{-1}. \tag{1}$$

At low temperatures the $T_{1d}^{-1}$-term is negligible, and the sum of $T_{1e}^{-1}$ and $T_{1p}^{-1}$ can be determined directly from $T_1^{-1}$-measurements. For the systems containing abundant metal nuclei with large quadrupole moments, an additional complication may arise from the cross-relaxation between proton and quadrupolar nuclear spins [20]. The cross-relaxation contribution to the proton relaxation rate, $T_{1c}^{-1}$, becomes important when the resonance frequency of a proton coincides with some resonance frequency (resulting from the combined quadrupole–Zeeman splitting) of a nearby metal nuclear spin, *and* H motion is frozen on the NMR frequency scale. If the proton resonance frequency is much higher than the highest nuclear-quadrupole-resonance (NQR) frequency of the metal spin system, the cross-relaxation contribution can be neglected. This contribution is also expected to be averaged out by H motion [20]. In our case, $^{93}$Nb nuclei (with the spin $I = 9/2$, the quadrupole moment $Q = -0.36$ b and 100% natural abundance) may, in principle, be responsible for the cross-relaxation contribution to the proton $T_1^{-1}$. According to the $^{93}$Nb NQR measurements [21], for $Nb_3Al$ the highest NQR frequency is 18.85 MHz. Hydrogen absorption has been reported to result in a significant reduction of the quadrupole coupling constant for $^{93}$Nb in $Nb_3Al$ [22], the highest NQR frequency for $Nb_3AlH_{2.2}$ being about 8 MHz. Therefore, following the arguments of reference [20], we can conclude that at the frequency of 90 MHz the cross-relaxation contribution to the measured proton $T_1^{-1}$ for our samples should be negligible. The low-temperature part of the temperature dependence of $T_1^{-1}$ measured at 90 MHz is shown in figure 4. At $T \leqslant 123$ K for $Nb_3AlH_{0.13}$ and at $T \leqslant 82$ K for $Nb_3AlH_{1.77}$ and $Nb_3AlH_{2.75}$ this

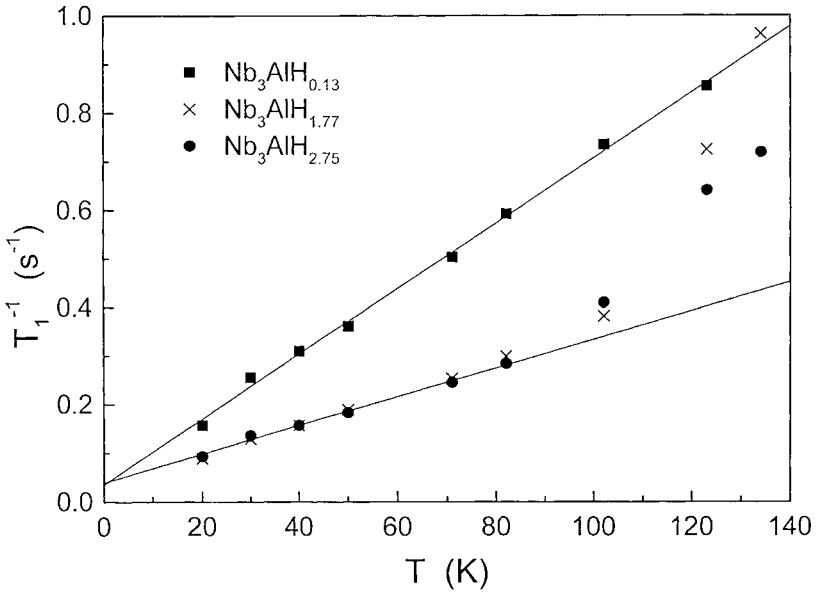


**Figure 4.** The low-temperature part of the temperature dependence of the proton spin–lattice relaxation rates for $Nb_3AlH_x$ at 90 MHz. The solid lines represent the fits of equation (2) to the data for $Nb_3AlH_{0.13}$ (at $T \leqslant 123$ K) and for $Nb_3AlH_{2.75}$ (at $T \leqslant 82$ K).

temperature dependence is well described by the linear function

$$(T_1^{-1})_{\mathrm{LT}} = R_e T + B. \tag{2}$$

Such a behaviour is typical of $T_{1e}^{-1} + T_{1p}^{-1}$ for systems with low impurity concentrations [12]. The fitted values of $R_e = (T_{1e}T)^{-1}$ characterizing the electronic (Korringa) contribution are $(6.7 \pm 0.1) \times 10^{-3}$, $(3.27 \pm 0.08) \times 10^{-3}$ and $(3.0 \pm 0.1) \times 10^{-3}$ $\mathrm{s}^{-1}$ $\mathrm{K}^{-1}$ for $x = 0.13$, 1.77 and 2.75, respectively. For transition-metal hydrides, $R_e$ is believed to be proportional to the square of the density of d-electron states at the Fermi level, $N_d^2(E_F)$ [23]. Therefore, the observed decrease in $R_e$ with increasing H content in $Nb_3AlH_x$ can be attributed to the decrease in $N_d(E_F)$. Similar behaviour of $R_e$ as a function of H concentration has been found for a number of other A15-type compounds with hydrogen [13–15]. The fitted values of $B$ for our $Nb_3AlH_x$ samples appear to be nearly the same, $B \approx 0.035$ $\mathrm{s}^{-1}$. At $T > 100$ K we observe strong deviations of the measured proton relaxation rates for $Nb_3AlH_{1.77}$ and $Nb_3AlH_{2.75}$ from the linear temperature dependence described by equation (2). For $Nb_3AlH_{0.13}$ such a deviation occurs above 140 K. These deviations should be ascribed to the dipole contribution $T_{1d}^{-1}$ resulting from the onset of H motion on the relevant frequency scale. Note that for $Nb_3AlH_x$ the temperatures at which this motional contribution to $T_1^{-1}$ becomes important are quite low. The dipole contribution to the relaxation rate can be evaluated by subtracting $T_{1e}^{-1} + T_{1p}^{-1}$ from the measured $T_1^{-1}$. Since the electronic contribution is frequency independent and $T_{1p}^{-1}$ is quite small, we may use the sum $T_{1e}^{-1} + T_{1p}^{-1}$ (obtained from the measurements at 90 MHz) for subtraction from the data at all frequencies. The temperature dependences of $T_{1d}^{-1}$ resulting from such a subtraction for $Nb_3AlH_{0.13}$ and $Nb_3AlH_{2.75}$ are shown in figures 5 and 6. It should be kept in mind, however, that at low frequencies (13 and 23.8 MHz) the $T_{1d}^{-1}$-values obtained in this way may also contain a certain cross-relaxation contribution at the low-temperature end. For the simplest Bloembergen–Purcell–Pound (BPP) model [24], the dipole contribution

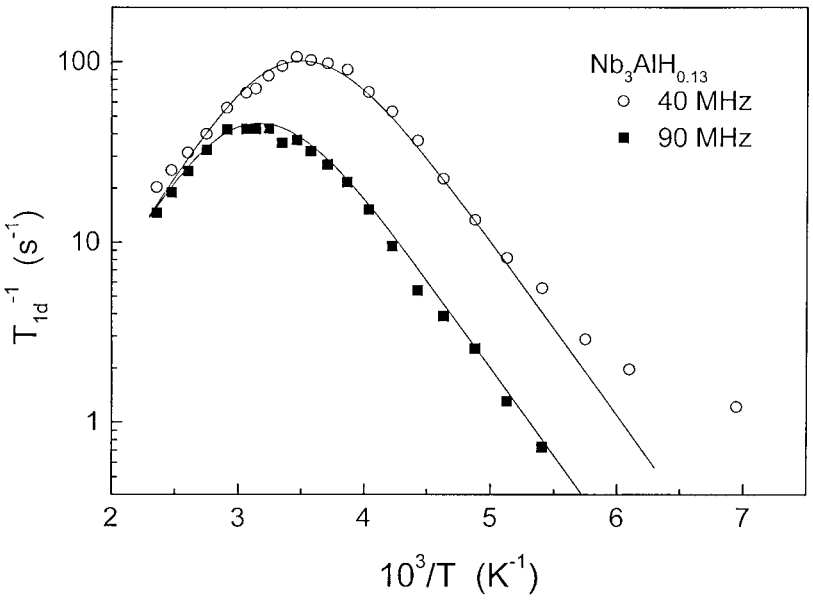


**Figure 5.** Dipolar contributions to the proton spin–lattice relaxation rate for $Nb_3AlH_{0.13}$ at 40 and 90 MHz as functions of reciprocal temperature. The points are obtained by subtracting the contributions of electronic origin (equation (2)) from the measured relaxation rates. The solid curves represent the simultaneous fit of the BPP model with the distribution of activation energies (equations (8), (3) and (7)) to the data at $T \geqslant 185$ K.

to the proton relaxation rate for $Nb_3AlH_x$ resulting from the $^1$H–$^1$H, $^1$H–$^{93}$Nb and $^1$H–$^{27}$Al interactions is given by

$$T_{1d}^{-1} = (T_{1d}^{-1})_{HH} + (T_{1d}^{-1})_{HNb} + (T_{1d}^{-1})_{HAl} = \frac{4M_{2HH}}{3\omega_H}\left[\frac{y}{4+y^2} + \frac{y}{1+y^2}\right] + \frac{M_{2HNb}}{2\omega_H}\left[\frac{y}{1+(1-b)^2y^2} + \frac{3y}{1+y^2} + \frac{6y}{1+(1+b)^2y^2}\right] + \frac{M_{2HAl}}{2\omega_H}\left[\frac{y}{1+(1-c)^2y^2} + \frac{3y}{1+y^2} + \frac{6y}{1+(1+c)^2y^2}\right]. \quad (3)$$

Here $y = \omega_H\tau_d$, $\tau_d$ is the mean time between two successive jumps of a hydrogen atom, and $M_{HH}$, $M_{HNb}$ and $M_{HAl}$ are the contributions to the 'rigid-lattice' second moment of the $^1$H NMR line from the corresponding dipole–dipole interactions:

$$M_{2HH} = \frac{3}{5}\gamma_H^4\hbar^2 I_H(I_H+1)\frac{x}{3}\sum_i r_i^{-6} \quad (4)$$

$$M_{2HNb} = \frac{4}{15}\gamma_H^2\gamma_{Nb}^2\hbar^2 I_{Nb}(I_{Nb}+1)\sum_j r_j^{-6} \quad (5)$$

$$M_{2HAl} = \frac{4}{15}\gamma_H^2\gamma_{Al}^2\hbar^2 I_{Al}(I_{Al}+1)\sum_k r_k^{-6} \quad (6)$$

where $I_H$, $I_{Nb}$ and $I_{Al}$ are the spins and $\gamma_H$, $\gamma_{Nb}$ and $\gamma_{Al}$ are the gyromagnetic ratios for $^1$H, $^{93}$Nb and $^{27}$Al, respectively, $b = \gamma_{Nb}/\gamma_H$ and $c = \gamma_{Al}/\gamma_H$. The summations $\sum_i r_i^{-6}$, $\sum_j r_j^{-6}$ and

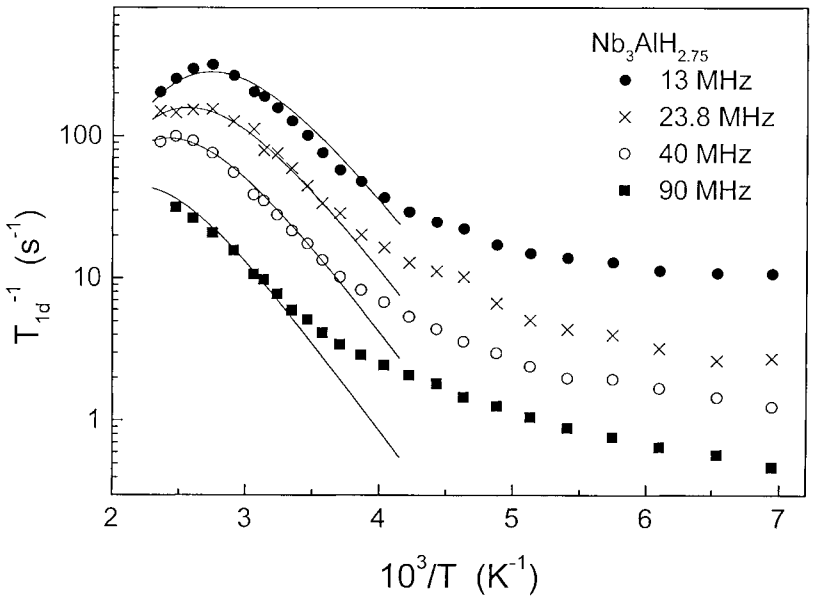


**Figure 6.** Dipolar contributions to the proton spin–lattice relaxation rate for $Nb_3AlH_{2.75}$ at 13, 23.8, 40 and 90 MHz as functions of reciprocal temperature. The points are obtained by subtracting the contributions of electronic origin (equation (2)) from the measured relaxation rates. The solid curves represent the simultaneous fit of the BPP model with the distribution of activation energies (equations (8), (3) and (7)) to the data at $T \geqslant 270$ K.

$\sum_k r_k^{-6}$ refer to sums over all H, Nb and Al sites, respectively, with the origin at a hydrogen site. The factor $x/3$ in equation (4) is the probability that a 6d site in $Nb_3AlH_x$ is occupied by a hydrogen atom. According to equation (3), in the limit of fast diffusion ($y \ll 1$) the value of $T_{1d}^{-1}$ is proportional to $\tau_d$, and in the limit of slow diffusion ($y \gg 1$) the value of $T_{1d}^{-1}$ is proportional to $\omega_H^{-2}\tau_d^{-1}$. It should be noted that more accurate lattice-specific Monte Carlo calculations of $T_{1d}^{-1}$ (see, e.g., [25]) lead to results that are close to the BPP predictions. In particular, the asymptotic behaviour of $T_{1d}^{-1}$ in the limits of fast and slow diffusion appears to be the same as in the BPP model. If $\tau_d$ follows the Arrhenius relation

$$\tau_d = \tau_{d0} \exp(E_a/k_B T) \tag{7}$$

where $E_a$ is the activation energy for hydrogen diffusion, then a plot of $\log T_{1d}^{-1}$ versus $T^{-1}$ is expected to be linear both in the fast-diffusion and slow-diffusion limits with the slopes $E_a/k_B$ and $-E_a/k_B$, respectively. However, the observed behaviour of $T_{1d}^{-1}$ for $Nb_3AlH_x$ deviates from the predictions of this simple model, the deviations being especially pronounced for $x = 1.77$ and 2.75. The observed frequency dependence of $T_{1d}^{-1}$ at low temperatures is weaker than $\omega_H^{-2}$. Moreover, there is a break in the slope of the $\log T_{1d}^{-1}$ versus $T^{-1}$ plots at low temperatures (figure 6). Note that the break is well pronounced even at the frequency of 90 MHz at which the cross-relaxation contribution should be negligible. In order to account for such features of the data as the weak frequency dependence of $T_{1d}^{-1}$ at low $T$ and the asymmetry of the $\log T_{1d}^{-1}$ versus $T^{-1}$ plots, one may use the model employing a distribution of values of $\tau_d$ (or $E_a$) [26, 27]. In this case the dipole contribution to the relaxation rate is calculated as

$$T_{1d}^{-1} = \int T_{1d}^{-1}(E_a) G(E_a)\, \mathrm{d}E_a \tag{8}$$

where $G(E_a)$ is the normalized distribution of $E_a$-values, and $T_{1d}^{-1}(E_a)$ is defined by equations (3) and (7). For parametrization of the data near the relaxation rate maximum we have used a Gaussian distribution function $G(E_a)$. The values of $M_{2HH}$ calculated from equation (4) are $1.67 \times 10^8$, $1.90 \times 10^9$ and $2.95 \times 10^9$ s$^{-2}$ for $x = 0.13$, 1.77 and 2.75, respectively. These values have been fixed in our analysis, each of them being at least an order of magnitude smaller than the corresponding value of $M_{2HNb}$. Since the values of $b$ and $c$ in equation (3) are close to each other, the second and the third terms in this equation show nearly the same temperature and frequency dependences. By introducing $M_{2HM} = M_{2HNb} + M_{2HAl}$, we can combine these terms. Therefore, the parameters of our model are $M_{2HM}$, $\tau_{d0}$, the average activation energy $\overline{E_a}$ and the distribution width $\Delta E_a$ (full width at half-maximum). These parameters are varied to find the best fit to the $T_{1d}^{-1}(T)$ data at all frequencies simultaneously. Since the model with a Gaussian shape of $G(E_a)$ cannot describe the low-temperature break in the slope of the $\log T_{1d}^{-1}$ versus $T^{-1}$ plots, the corresponding low-$T$ region has been excluded from the fitting. The results of the fits are shown as solid curves in figures 5 and 6, and the fit parameters are listed in table 1.

**Table 1.** Parameters resulting from the fits of the BPP model with a Gaussian distribution of activation energies to the high-temperature $T_1^{-1}$-data.

| Sample | $M_{2HM}$ ($s^{-2}$) | $\tau_{d0}$ (s) | $\overline{E_a}$ (eV) | $\Delta E_a$ (eV) |
|---|---|---|---|---|
| $Nb_3AlH_{0.13}$ | $1.3 \times 10^{10}$ | $8 \times 10^{-13}$ | 0.21 | 0.016 |
| $Nb_3AlH_{1.77}$ | $1.55 \times 10^{10}$ | $8 \times 10^{-13}$ | 0.30 | 0.043 |
| $Nb_3AlH_{2.75}$ | $1.3 \times 10^{10}$ | $8 \times 10^{-13}$ | 0.30 | 0.034 |

As can be seen from figure 5, for $Nb_3AlH_{0.13}$ the model gives a reasonable description of the data down to 185 K at two frequencies with the *same* set of parameters. Since for $Nb_3AlH_{1.77}$ and $Nb_3AlH_{2.75}$ the temperature of the relaxation rate maximum is close to the upper limit of our measurements, it is difficult to derive both $\tau_{d0}$ and $\overline{E_a}$ independently; therefore, the pre-exponential factor for these compounds has been fixed to the value $\tau_{d0} = 8 \times 10^{-13}$ s obtained for $Nb_3AlH_{0.13}$. The model describes the $T_{1d}^{-1}(T)$ data for $Nb_3AlH_{1.77}$ and $Nb_3AlH_{2.75}$ at four frequencies simultaneously down to approximately 270 K. As expected for the metal–hydrogen dipole–dipole contributions, the fitted values of $M_{2HM}$ for $Nb_3AlH_x$ are nearly $x$-independent. The average activation energy $\overline{E_a}$ for $Nb_3AlH_{0.13}$ is considerably lower than for the $Nb_3AlH_x$ samples with high hydrogen concentrations. The increase in the activation energy with increasing H content has also been reported for A15-type $Ti_3IrH_x$ (from 0.155 eV for $x = 0.55$ to 0.365 eV for $x = 3.0$) [13]. One of the factors responsible for such a concentration dependence of the activation energy may be the increase in the intersite distances with increasing $x$. The fitted values of $\Delta E_a$ for $Nb_3AlH_x$ appear to be small as compared to the corresponding values of $\overline{E_a}$. This means that the description of the data in the region of the relaxation rate maxima does not require broad $E_a$-distributions. As noted above, the model with a Gaussian (or other single-peak) distribution of $E_a$-values cannot account for the low-$T$ break in the slope of the $\log T_{1d}^{-1}$ versus $T^{-1}$ plots. This feature can be described by the BPP model with a bimodal distribution of $E_a$-values [28]. Such a distribution implies two frequency scales of H hopping. If these two frequency scales are well separated from each other, the temperature dependence of $T_{1d}^{-1}$ shows two peaks [29, 30]. In other cases, the presence of the second frequency scale of H hopping can lead to a weak temperature dependence of $T_{1d}^{-1}$ at low $T$ [28, 31, 32]. For our $Nb_3AlH_x$ samples with $x = 1.77$ and 2.75, the low-$T$ break in the slope of the $\log T_{1d}^{-1}$ versus $T^{-1}$ plots may be attributed to the second frequency scale of H

motion. The coexistence of two types of H hopping with different frequency scales has been confirmed by recent quasielastic neutron scattering measurements on $Nb_3AlH_x$ [33]. In order to discuss the origin of the two frequency scales of H hopping for A15-type compounds, let us consider the sublattice of d sites partially occupied by hydrogen atoms. The unit cell of the A15-type lattice with d sites is shown in figure 7. The sublattice of d sites is identical to the sublattice of A atoms. These sites form three sets of non-intersecting chains in the $\langle 100\rangle$, $\langle 010\rangle$ and $\langle 001\rangle$ directions. The distance between the nearest-neighbour d sites in the chains, $r_1 = a_0/2$, is 22% shorter than the shortest distance between d sites on different chains, $r_2 = \sqrt{3}a_0/2\sqrt{2}$. Since H hopping rates in intermetallics strongly depend on distances between the corresponding sites [34,35], a hydrogen atom is expected to perform many jumps along a chain before it jumps to another chain. Thus, the structure of the d-site sublattice in A15-type compounds suggests the possibility of two frequency scales of H hopping, the faster jump process corresponding to the motion along the chain. Note that for high H concentrations ($x > 1.5$) the hopping along the chain may be considered as a nearly localized motion. In fact, if the d-site sublattice is more than half-filled, the motion of H atoms along the chain should be dominated by back-and-forth jumps within pairs of the nearest-neighbour sites.

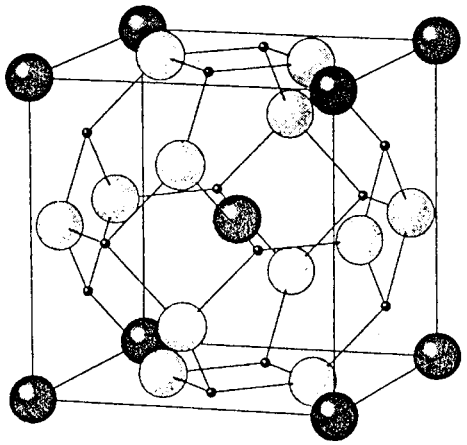

**Figure 7.** The unit cell of the A15-type lattice with interstitial d sites (from [19]). Open circles: A atoms; filled circles: B atoms; small filled circles: d sites.

## 4. Conclusions

The results of our measurements of the proton spin–lattice relaxation rate $T_1^{-1}$ for A15-type $Nb_3AlH_x$ can be summarized as follows.

(1) The electronic (Korringa) contribution to the relaxation rate, $(T_{1e}T)^{-1}$, is found to decrease with increasing H content from $6.7 \times 10^{-3}$ s$^{-1}$ K$^{-1}$ for $x = 0.13$ to $3.0 \times 10^{-3}$ s$^{-1}$ K$^{-1}$ for $x = 2.75$.

(2) The hydrogen hopping rate estimated from the high-temperature $T_1^{-1}$-data decreases with increasing H content. The corresponding effective activation energies for hydrogen diffusion are 0.21 eV for $x = 0.13$ and 0.30 eV for $x = 1.77$ and 2.75.

(3) At low temperatures ($T < 270$ K for $x = 1.77$ and 2.75) the proton relaxation rate shows strong deviations from the predictions of the simple model with a single-peak distribution of activation energies.

Such a behaviour suggests a coexistence of at least two frequency scales of H hopping. The interstitial d sites partially occupied by H atoms in $Nb_3AlH_x$ form three sets of non-intersecting chains, the distance between the nearest-neighbour d sites in the chains being 22% shorter than the shortest distance between d sites on different chains. Thus, the structure of the d-site sublattice is consistent with the coexistence of two characteristic jump rates for H atoms. This feature may also explain the earlier observations [14, 15] of two frequency scales of H hopping in A15-type compounds.

## Acknowledgment

This work was partially supported by the Russian Foundation for Basic Research (Grant No 99-02-16311).

## References

[1] Vonsovsky S V, Izyumov Yu A and Kurmaev E Z 1982 *Superconductivity of Transition Metals, Their Alloys and Compounds* (Berlin: Springer)
[2] Muller J 1980 *Rep. Prog. Phys.* **43** 641
[3] Sahm P R 1968 *Phys. Lett.* A **26** 459
[4] Vieland L J, Wicklund A W and White J G 1975 *Phys. Rev.* B **11** 3311
[5] Shamrai V F and Padurets L N 1979 *Dokl. Acad. Nauk SSSR* **246** 1182
[6] Huang S Z, Skoskiewicz T, Chu C W and Smith J L 1980 *Phys. Rev.* B **22** 137
[7] Rama Rao K V S, Mrowietz M and Weiss A 1982 *Ber. Bunsenges. Phys. Chem.* **86** 1135
[8] Antonov V E, Antonova T E, Belash I T, Zharikov O V, Latynin A I, Palnichenko A V and Rashchupkin V I 1989 *Sov. Phys.–Solid State* **31** 1659
[9] Schlereth M and Wipf H 1990 *J. Phys.: Condens. Matter* **2** 6927
[10] Baier M, Wordel R, Wagner F E, Antonova T E and Antonov V E 1991 *J. Less-Common Met.* **172** 358
[11] Rama Rao K V S, Sturm H, Elschner B and Weiss A 1983 *Phys. Lett.* A **93** 492
[12] Barnes R G 1997 *Hydrogen in Metals III* ed H Wipf (Berlin: Springer) p 93
[13] Guthardt D, Beisenherz D and Wipf H 1992 *J. Phys.: Condens. Matter* **4** 6919
[14] Skripov A V, Belyaev M Yu and Petrova S A 1992 *J. Phys.: Condens. Matter* **4** L537
[15] Skripov A V, Cherepanov Yu G and Wipf H 1994 *J. Alloys Compounds* **209** 111
[16] Yvon K and Fischer P 1988 *Hydrogen in Intermetallic Compounds I* ed L Schlapbach (Berlin: Springer) p 87
[17] Skripov A V, Podlesnyak A A and Fischer P 1994 *J. Alloys Compounds* **210** 27
[18] Cornell K, Wipf H, Stuhr U and Skripov A V 1997 *Solid State Commun.* **101** 569
[19] Antonov V E, Bokhenkov E L, Dorner B, Fedotov V K, Grosse G, Latynin A I, Wagner F E and Wordel R 1998 *J. Alloys Compounds* **264** 1
[20] Lichty L R, Han J W, Torgeson D R, Barnes R G and Seymour E F W 1990 *Phys. Rev.* B **42** 7734
[21] Matukhin V L, Saikin K S and Safin I A 1977 *Fiz. Tverd. Tela* **19** 1161
[22] Matukhin V L 1980 *PhD Thesis* Kazan Physico-Technical Institute, Kazan
[23] Cotts R M 1978 *Hydrogen in Metals I* ed G Alefeld and J Völkl (Berlin: Springer) p 227
[24] Bloembergen N, Purcell E M and Pound R M 1948 *Phys. Rev.* **73** 679
[25] Faux D A, Ross D K and Sholl C A 1986 *J. Phys. C: Solid State Phys.* **19** 4115
[26] Shinar J, Davidov D and Shaltiel D 1984 *Phys. Rev.* B **30** 6331
[27] Markert J T, Cotts E J and Cotts R M 1988 *Phys. Rev.* B **37** 6446
[28] Skripov A V, Rychkova S V, Belyaev M Yu and Stepanov A P 1989 *Solid State Commun.* **71** 1119
[29] Skripov A V, Rychkova S V, Belyaev M Yu and Stepanov A P 1990 *J. Phys.: Condens. Matter* **2** 7195
[30] Skripov A V, Soloninin A V, Stepanov A P and Kozhanov V N 1999 *J. Phys.: Condens. Matter* **11** 10 393
[31] Bowman R C, Craft B D, Attalla A and Johnson J R 1983 *Int. J. Hydrogen Energy* **8** 801
[32] Skripov A V and Belyaev M Yu 1993 *J. Phys.: Condens. Matter* **5** 4767
[33] Skripov A V, Combet J, Hempelmann R and Kozhanov V N 2000 to be published
[34] Skripov A V, Cook J C, Sibirtsev D S, Karmonik C and Hempelmann R 1998 *J. Phys.: Condens. Matter* **10** 1787
[35] Skripov A V, Pionke M, Randl O and Hempelmann R 1999 *J. Phys.: Condens. Matter* **11** 1489